First investigation of fast-ion-driven modes in Wendelstein 7-X

C. Slaby[1], S. Äkäslompolo[1], M. Borchardt[1], J. Geiger[1], R. Kleiber[1], A. Könies[1], S. Bozhenkov[1], C. Brandt[1], A. Dinklage[1], M. Dreval[2], G. Fuchert[1], D. Hartmann[1], M. Hirsch[1], U. Höfel[1], P. McNeely[1], N. Pablant[3], K. Rahbarnia[1], N. Rust[1], J. Schilling[1], A. von Stechow[1], H. Thomsen[1], and the W7-X Team[4]

[1] Max Planck Institute for Plasma Physics, Wendelsteinstr. 1, 17491 Greifswald, Germany
[2] Kharkov Institute of Physics and Technology, 1, Akademicheskaya St., Kharkov, 61108, Ukraine
[3] Plasma Physics Laboratory, Princeton University, PO Box 451, Princeton, NJ 08543, USA
[4] see author list of T. Klinger et al., Nucl. Fusion **59** 112004 (2019)

September 5, 2019

This work has been carried out within the framework of the EUROfusion Consortium and has received funding from the Euratom research and training programme 2014-2018 and 2019-2020 under grant agreement No 633053. The views and opinions expressed herein do not necessarily reflect those of the European Commission.

Motivation

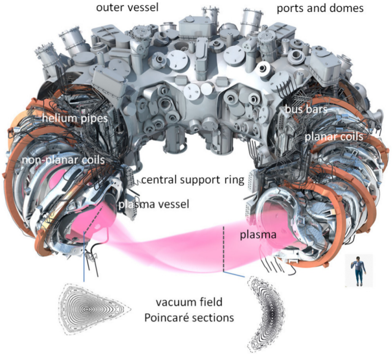

T. Klinger et al.,Plasma Phys. Control. Fusion **59** 014018 (2017)

- W7-X is a large optimized stellarator
- included in the optimization criteria were good fast-ion confinement and MHD stability
- fast ions can increase heat loads on vessel walls (see P2-23 by S. Äkäslompolo)
- fast ions can interact with MHD modes (Alfvén eigenmodes)

⇒ energy losses can be the consequence

Goals of this presentation:

- show progress of data evaluation tools
- theoretical explanation of experimentally observed mode activity

⇒ validate our numerical tools

As this is the first attempt of this complex task for W7-X, a number of challenges remain for the future.

Fast ions at the Wendelstein 7-X stellarator

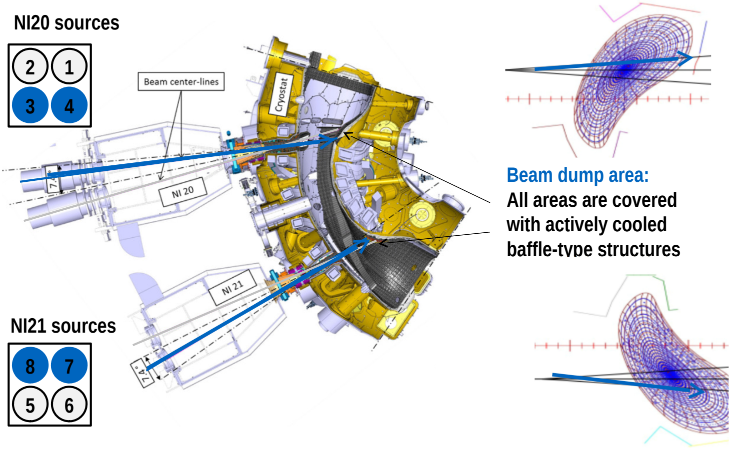

- last operation phase of W7-X (OP 1.2b from July till October 2018) featured, for the first time, NBI to generate fast ions
- NBI injected protons with an energy of $55\ \mathrm{keV}$
- normalized gyroradius matches that of alpha particles in ITER

Experimental observations in OP 1.2b

MHD mode activity has been observed in a number of discharges

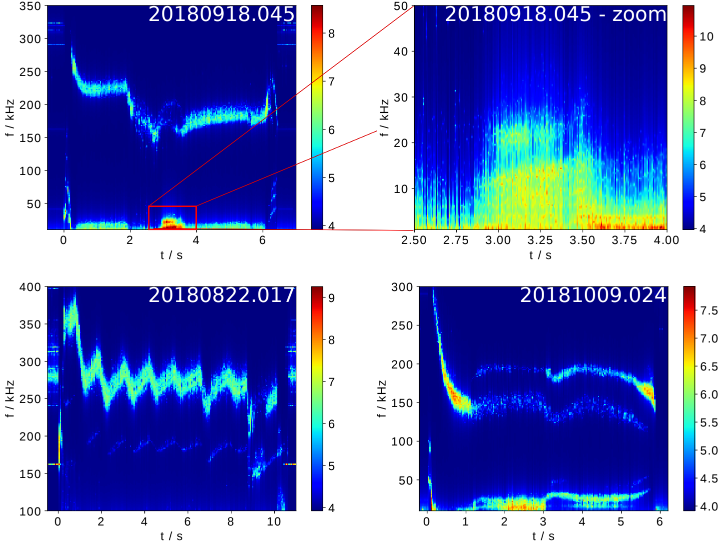

- wealth of data which needs to be evaluated (not all related to fast ions)

Contents

Contents

Advanced signal processing

DMUSIC

- accurate extraction of mode frequencies from experimental data
- in contrast to FFT: parametric method
- assumes a system of exponentially damped modes

$$\hat{y}(n) = \sum_{i=1}^{K} a_i \exp[s_i n] \qquad s_i \in \mathbb{C}$$

- linear prediction ansatz

$$y(n) = \sum_{i=1}^{J} c_{J-i} y(n-i)$$

- frequency resolution not limited

$\Rightarrow$ signals can be seen more clearly than in a standard FFT

Data evaluation: DMUSIC

- power of DMUSIC[1,2] can clearly be seen when calculating continuum from gyrokinetic particle simulation

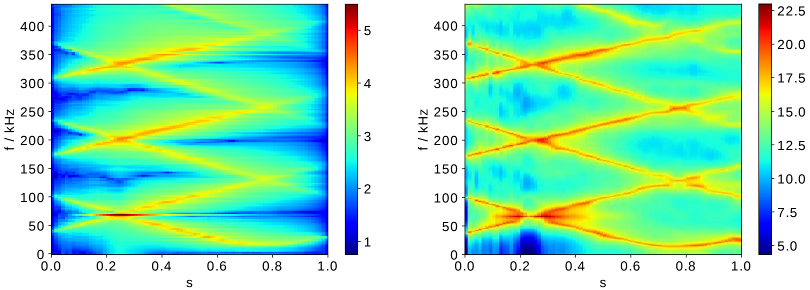

with FFT

with DMUSIC

- ITPA benchmark case (circular tokamak, $n = -6$ TAE)
- gyrokinetic simulation with EUTERPE
- the same tool is used for the spectrograms shown here (just exchange radial coordinate with time)

[1] Y. Li et al., Institute for Systems Research T.R. 95-11 (1995)

[2] Y. Li et al., IEEE T BIO-MED ENG **45** 78–86 (1998)

Advanced signal processing

DMUSIC

- accurate extraction of mode frequencies from experimental data
- in contrast to FFT: parametric method
- assumes a system of exponentially damped modes

$$\hat{y}(n) = \sum_{i=1}^{K} a_i \exp[s_i n] \qquad s_i \in \mathbb{C}$$

- linear prediction ansatz

$$y(n) = \sum_{i=1}^{J} c_{J-i} y(n-i)$$

- frequency resolution not limited

⇒ signals can be seen more clearly than in a standard FFT

Stochastic System Identification

- determination of mode frequencies and structures from array of signals

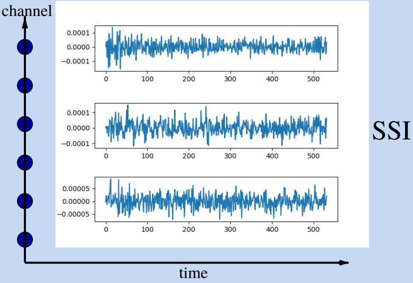

$$\mathbf{x}_{k+1} = A\mathbf{x}_k + \mathbf{w}_k$$
$$\mathbf{y}_{k+1} = C\mathbf{x}_k + \mathbf{v}_k$$

- $\mathbf{y}_k$: observables
- $\mathbf{x}_k$: hidden dynamic system
- $\mathbf{w}_k, \mathbf{v}_k$: noise

DMUSIC

- accurate extraction of mode frequencies from experimental data
- in contrast to FFT: parametric method
- assumes a system of exponentially damped modes

$$\hat{y}(n) = \sum_{i=1}^{K} a_i \exp[s_i n] \qquad s_i \in \mathbb{C}$$

- linear prediction ansatz

$$y(n) = \sum_{i=1}^{J} c_{J-i} y(n-i)$$

- frequency resolution not limited

$\Rightarrow$ signals can be seen more clearly than in a standard FFT

Stochastic System Identification

- determination of mode frequencies and structures from array of signals

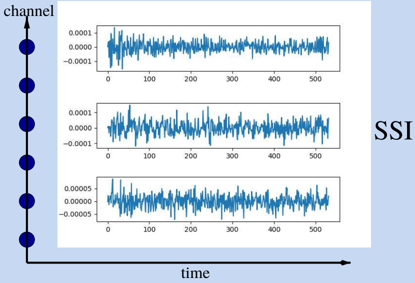

$$\mathbf{x}_{k+1} = A\mathbf{x}_k + \mathbf{w}_k$$
$$\mathbf{y}_{k+1} = C\mathbf{x}_k + \mathbf{v}_k$$

- system frequencies: eigenvalues of A
- eigenmodes: $C \cdot$ (eigenvectors of A)

Data evaluation: Stochastic System Identification (SSI)

- SSI method[3] allows determination of mode frequencies and structures from array of time signals

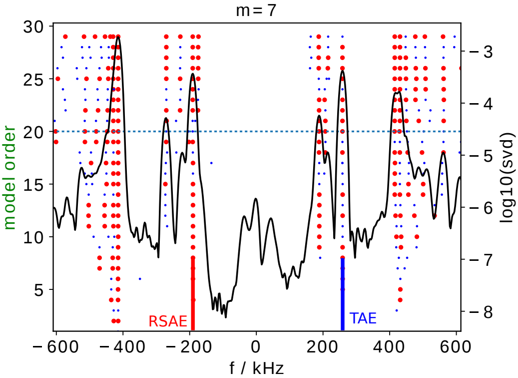

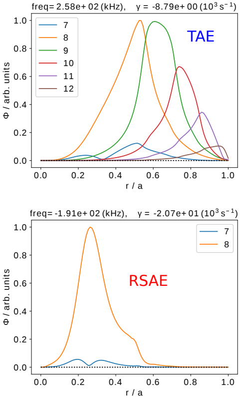

- can separate TAE and RSAE in gyrokinetic EUTERPE simulation of circular tokamak

[3] B. Peeters et al., J. Dyn. Sys., Meas., Control **123** 659–667 (2001)

Contents

Observations in experimental programme 20181009.024

- for this investigation: focus on NBI-discharge with diverse mode activity

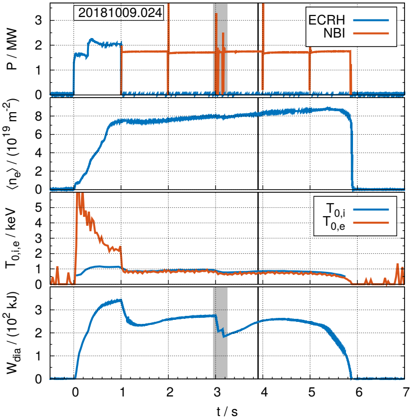

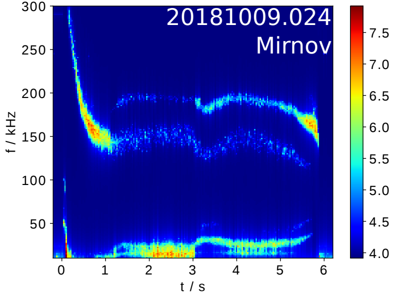

- NBI-dominated discharge with ECRH start-up
- NBI sources switched each second

- mode activity observed by Mirnov coils, PCI, and XMCTS
- very obvious: AEs at different frequencies are observed
- hypothesis: Mirnov coils see edge-localized EAEs where PCI and XMCTS observe core-localized modes

Observations in experimental programme 20181009.024

- for this investigation: focus on NBI-discharge with diverse mode activity

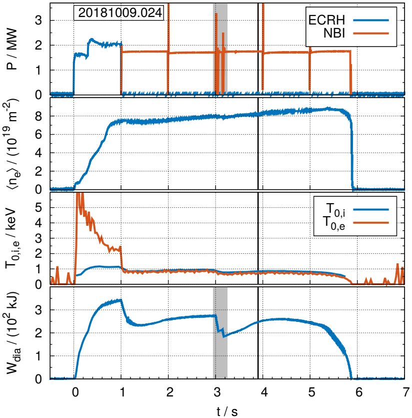

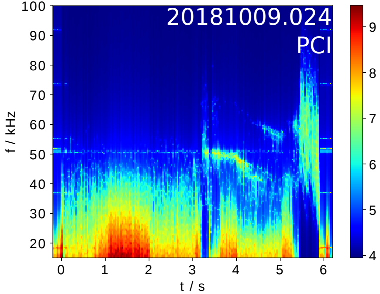

- NBI-dominated discharge with ECRH start-up
- NBI sources switched each second

- mode activity observed by Mirnov coils, PCI, and XMCTS
- very obvious: AEs at different frequencies are observed
- hypothesis: Mirnov coils see edge-localized EAEs where PCI and XMCTS observe core-localized modes

Observations in experimental programme 20181009.024

- for this investigation: focus on NBI-discharge with diverse mode activity

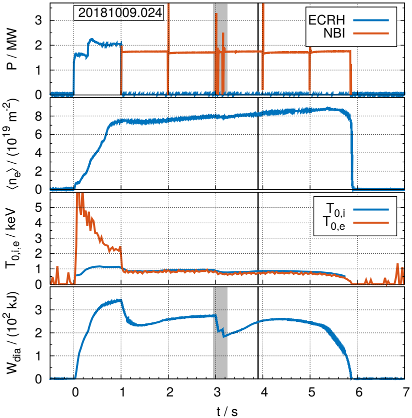

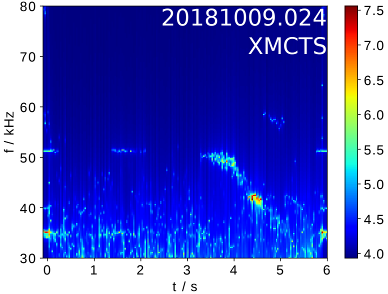

- NBI-dominated discharge with ECRH start-up
- NBI sources switched each second

- mode activity observed by Mirnov coils, PCI, and XMCTS
- very obvious: AEs at different frequencies are observed
- hypothesis: Mirnov coils see edge-localized EAEs where PCI and XMCTS observe core-localized modes

Plasma profiles

- background plasma profiles needed for computation of shear Alfvén wave continua, MHD eigenmodes and fast-ion distribution function

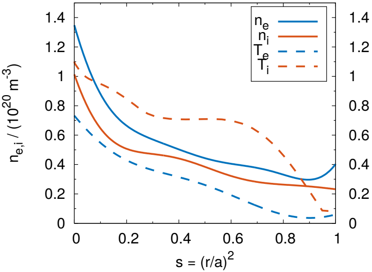

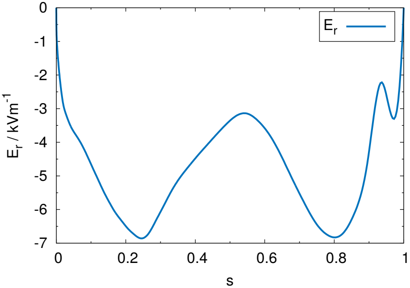

- cold discharge (NBI heating power is only $1.75\ \mathrm{MW}$)
- T_i probably higher than in the actual discharge (error in diagnostic)
- characteristic for NBI discharges in W7-X: strong fuelling $\rightarrow$ density peaks on axis
- E_r calculated by NTSS taking the profiles as input
- effects of radial electric field on shear Alfvén continuum will be discussed separately

Shear Alfvén wave continua I

- Shear Alfvén continua computed for the three mode families of W7-X

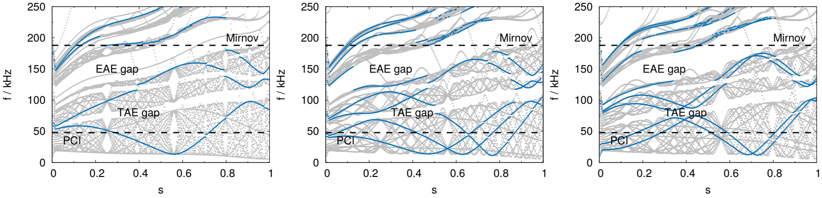

- SSI mode number analysis suggests modes with $m \in [10, 15] \rightarrow$ coloured branches (n is unknown)
- mode observed by Mirnov coils fits well into EAE gap
- TAE gap is (roughly) at the correct frequency in the core to match PCI and XMCTS data

$\Rightarrow$ continuum valuable for interpretation of experimental data

- slow-sound approximation used (good for frequencies around the EAE gap, not so good for the TAE gap)
- Doppler shift due to the presence of E_r neglected here

Shear Alfvén wave continua II: Full coupling to sound waves

- coupling to sound waves affects low-frequency branches in the Alfvén continuum

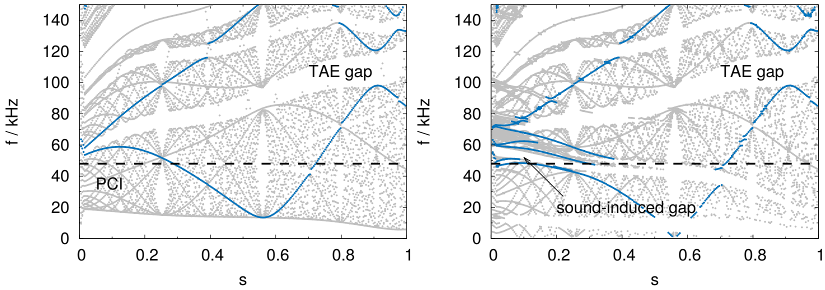

($N = 0$ mode family)

- structure of the TAE gap changes in the core due to the coupling to sound waves
- sound-induced gap opens at around $50\ \mathrm{kHz}$ in the core
- position of this gap matches the frequencies observed by PCI and XMCTS
- in general for this case: background-plasma beta is low ($\langle\beta\rangle = 0.3\%$) $\rightarrow$ pressure effects not very pronounced
- higher-frequency EAE gap almost unaffected

Shear Alfvén wave continua III: Doppler shift due to E_r

- E_r exists in stellarators to ensure the overall ambipolarity of the neoclassical particle fluxes $\Rightarrow$ poloidal $\mathbf{E} \times \mathbf{B}$ rotation of the plasma

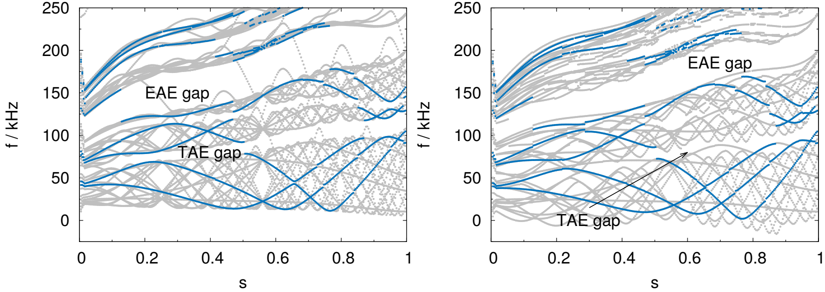

($N = 1$ mode family)

- Doppler shift can be estimated by

$$\Delta\omega = v_{\mathbf{E}\times\mathbf{B}} k_\perp \approx \frac{E_r}{B} \frac{m}{\sqrt{s}}$$

- frequency gaps remain open even after the shift is applied
- this is more clearly visible for the EAE gap than for the TAE gap
- frequency shift depends on radial location and mode numbers (but typical value in the range of $10\ \mathrm{kHz}$)

Discrete eigenmodes in frequency gaps of the spectrum

- the CKA code is used to compute discrete MHD eigenmodes in the frequency gaps of the continuous spectra

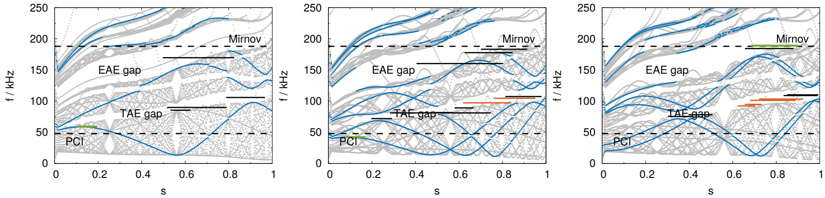

- 26 modes (spread over 3 mode families) in the frequency range of the experimental observations found

$\Rightarrow$ all of them have to be included as possible candidates in the kinetic simulations

- three types of modes found: GAEs, TAEs, and EAEs
- frequency of core-localized GAEs matches observations from PCI and XMCTS
- some of the edge-localized EAEs match the measurements by the Mirnov coils
- TAEs at around $100\ \mathrm{kHz}$ were not observed by any diagnostics

- Can these modes be destabilized by fast ions?

Discrete eigenmodes in frequency gaps of the spectrum

- the CKA code is used to compute discrete MHD eigenmodes in the frequency gaps of the continuous spectra

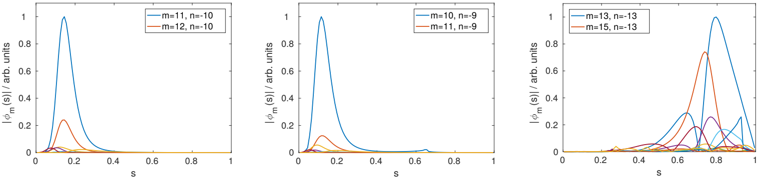

- 26 modes (spread over 3 mode families) in the frequency range of the experimental observations found

$\Rightarrow$ all of them have to be included as possible candidates in the kinetic simulations

- three types of modes found: GAEs, TAEs, and EAEs
- frequency of core-localized GAEs matches observations from PCI and XMCTS
- some of the edge-localized EAEs match the measurements by the Mirnov coils
- TAEs at around $100\ \mathrm{kHz}$ were not observed by any diagnostics

- Can these modes be destabilized by fast ions?

We need a fast-ion distribution function: use ASCOT

- the Monte-Carlo particle-following code ASCOT is used to calculate the fast-ion distribution function

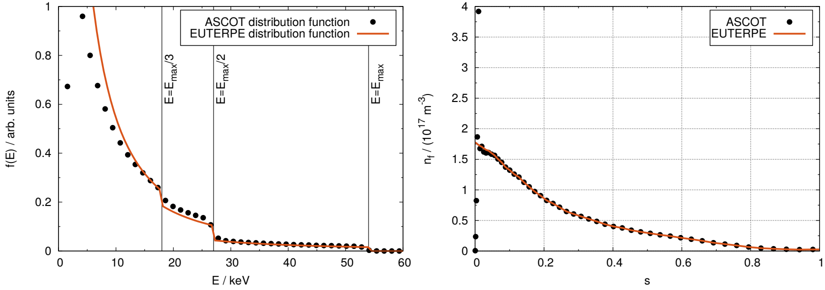

- anisotropic ASCOT distribution function used to estimate parameters of an isotropic model distribution function

$\Rightarrow$ more flexibility

- effects of velocity-space anisotropies can be studied separately
- input for the perturbative gyrokinetic code CKA-EUTERPE

$\Rightarrow$ numerically inexpensive, allows to assess the stability of many modes

Stability of the modes

- CKA-EUTERPE used to compute growth and damping rates of the modes (ions, electrons, or fast ions used as kinetic species)

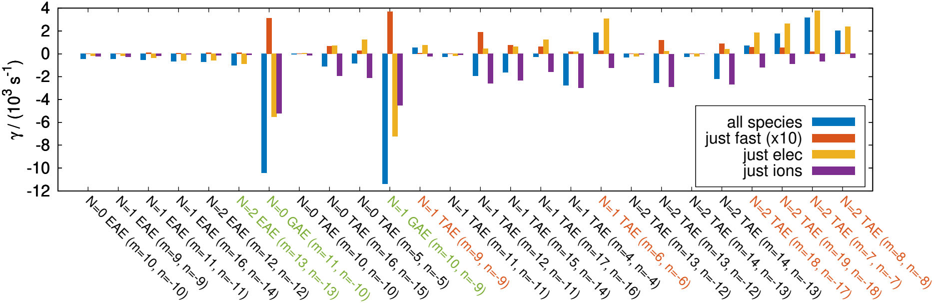

<u>CKA-EUTERPE paints an ambiguous picture:</u>

- in general: kinetic effects of background-plasma dominate over that of fast particles (understandable since fast-ion beta is low)
- some TAEs are destabilized by background-plasma electrons (but not observed by the diagnostics) ⇒ depends strongly on the profiles
- core-localized GAEs react most strongly to fast ions, but also have the strongest damping rates
- their frequencies agree with experimental measurements

Power transfer in phase space

- we can plot the resonant wave-particle power transfer in velocity space
- just the fast particles have been considered here

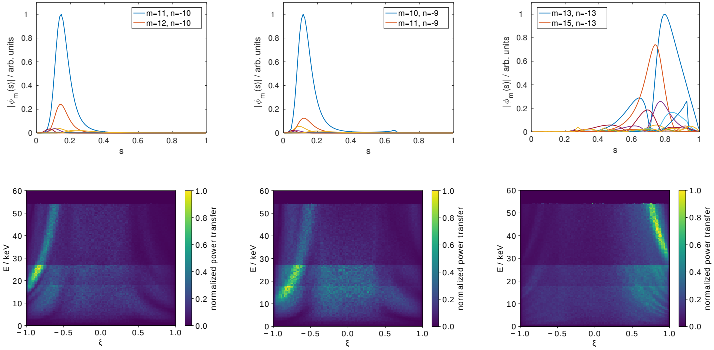

- core-GAEs driven by medium-energy counter-passing fast ions
- edge-EAE driven by high-energy co-passing particles

$\Rightarrow$ more fast ions available for the interaction with the GAEs

$\Rightarrow$ fast-ion density gradient stronger in the core

$\Rightarrow$ this explains the higher growth rates of the GAEs

$\Rightarrow$ we need passing particles, but typically f_0 peaks around $\xi = \pm 0.4$ in W7-X

Effects of an anisotropic fast-ion distribution function

- make distribution function progressively more anisotropic

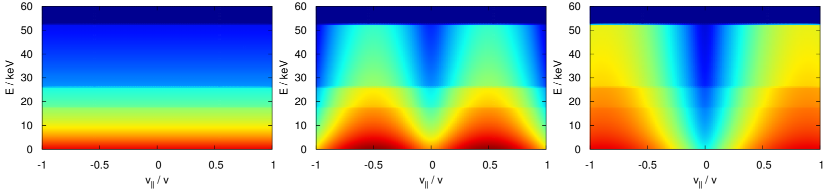

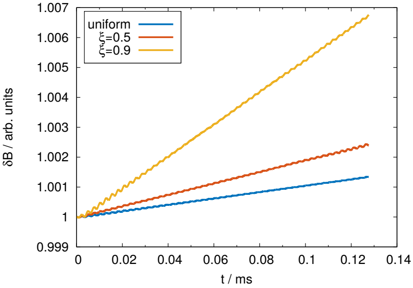

- an anisotropic distribution function leads to more particles in the resonant regions of phase space
- fast-ion drive can increase by up to 400% (for edge-EAE)
- indicates sensitivity of the results on parameters of the distribution function
- f_0 is still symmetric in ξ $\rightarrow$ no equilibrium current included in the modelling

Contents

Summary and conclusions

- OP 1.2b featured NBI heating and generation of fast ions
- MHD activity has been observed in a number of discharges from this campaign
- experimental data have been analysed with advanced signal processing tools (DMUSIC and SSI)
- we are in the process of validating our tools (CONTI–CKA–EUTERPE) with experimental data
- CKA-EUTERPE finds modes matching the experimental observations in frequency
- still a very hands-on process: more experimental guidance (in terms of mode numbers, radial location) would be helpful
- computing accurate growth/damping rates will require better knowledge of distribution functions and profiles (experimental challenge)

To be done:

- fully gyrokinetic EUTERPE simulations
- they are challenging due low fast-ion density and the resulting low growth rates

Back-up slides

Effect of new profiles I - profiles

profile type 1:

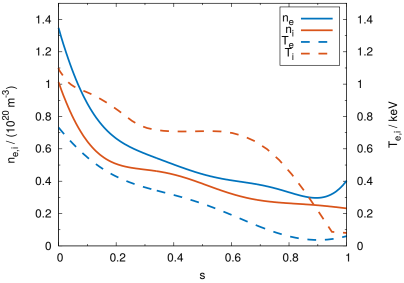

profile type 2:

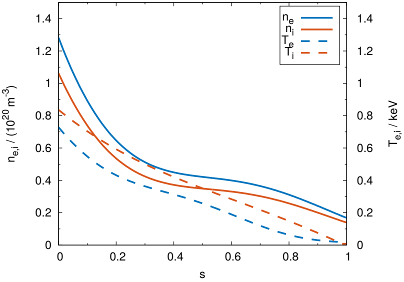

Effect of new profiles II - continua

profile type 1:

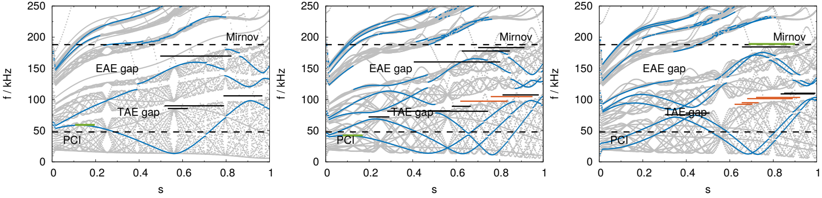

profile type 2:

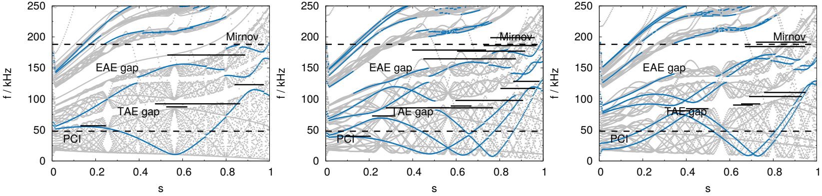

Effect of new profiles III - eigenmodes

profile type 1:

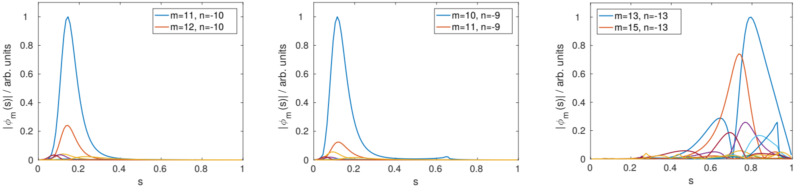

profile type 2:

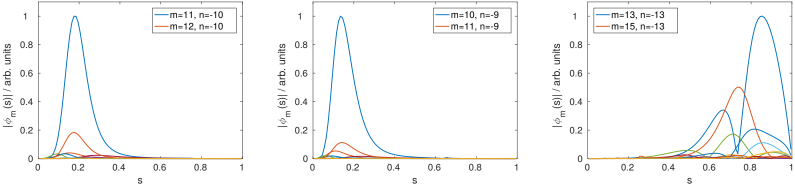

Effect of new profiles IV - kinetic drive

profile type 1:

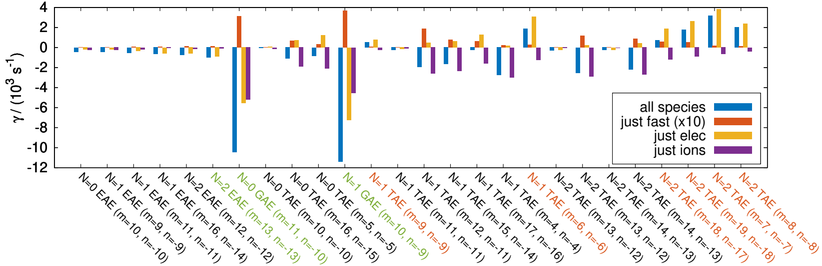

profile type 2:

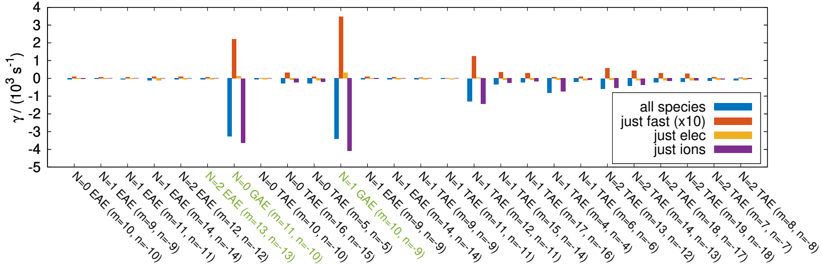

Data evaluation: Stochastic System Identification (SSI)

- SSI method allows determination of mode frequencies and structures from array of time signals

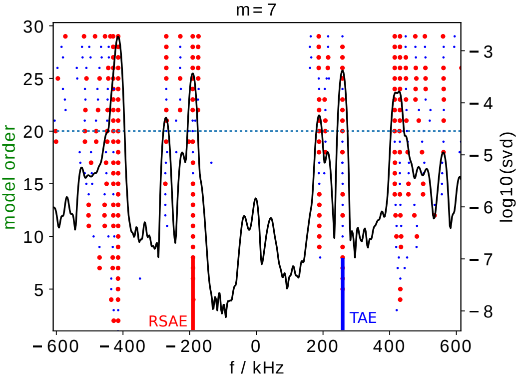

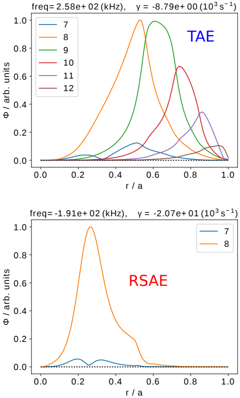

- can separate TAE and RSAE in gyrokinetic EUTERPE simulation of circular tokamak

Data evaluation: Stochastic System Identification (SSI)

- SSI method allows determination of mode frequencies and structures from array of time signals

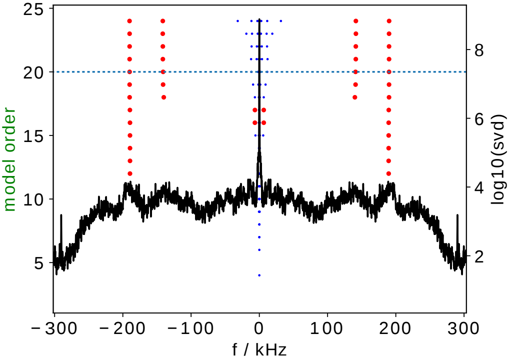

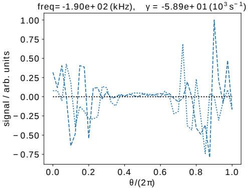

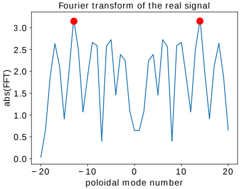

- can be applied to experimental data from Mirnov coils
- modes at $150\ \mathrm{kHz}$ and $190\ \mathrm{kHz}$ found (seen also in DMUSIC spectrogram)
- spacial mode structures and mode numbers have been extracted for the $190\ \mathrm{kHz}$ mode

The CKA-EUTERPE model

- perturbative model using mode structure and frequency determined by CKA as input
- Poisson equation and Ampère's law do not need to be solved
- instead: amplitudes of electromagnetic potentials evolved according to

$$\frac{\partial \hat{\phi}(t)}{\partial t} = \mathrm{i}\omega\left(\hat{A}_\parallel - \hat{\phi}\right) + 2\left(\gamma(t) - \gamma_\mathrm{d}\right)\hat{\phi}$$

$$\frac{\partial \hat{A}_\parallel(t)}{\partial t} = \mathrm{i}\omega\left(\hat{\phi} - \hat{A}_\parallel\right)$$

- damping rate is external parameter (can be specified using e.g. STAE-K[4])
- growth rate computed from power transfer of particles to mode

$$\gamma(t) = \frac{P(t)}{T}$$

$$P(t) = -\int \mathrm{d}\Gamma\, B_\parallel^\star \left[\frac{m}{ZeB}\mathbf{b} \times \left(v_\parallel^2 \boldsymbol{\kappa} + \mu\nabla B\right) \cdot \left(Ze\nabla_\perp \phi^*(\mathbf{r},t) f^{(1)}\right)\right]$$

$$T = \int \mathrm{d}^3 r\, \frac{m_\mathrm{i} n_\mathrm{i}}{2B^2} \left|\nabla_\perp \phi(\mathbf{r},t)\right|^2$$

$$\phi(\mathbf{r},t) = \hat{\phi}(t)\,\phi_0(\mathbf{r}) \exp(\mathrm{i}\omega t)$$

[4] C. Slaby et al., Phys. Plasmas **23** 092501 (2016)

Mode families in Wendelstein 7-X

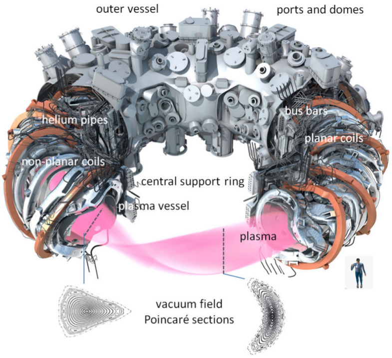

T. Klinger et al.,Plasma Phys. Control. Fusion **59** 014018 (2017)

- three independent mode families exist in W7-X
- consequence of the three-dimensional geometry of the plasma

⇒ not all toroidal modes can freely interact with each other

– $N = 0$ mode family

■ $N = 1$ mode family

○ $N = 2$ mode family

n	...	-7	-6	-5	-4	-3	-2	-1	0	1	2	3	4	5	6	7	...
family	...	○	■	–	■	○	○	■	–	■	○	○	■	–	■	○	...

- table adapted from[5]

[5] C. Schwab, Phys. Fluids B **5** 3195 (1993)